

## Many-Body Radiative Decay in Strongly Interacting Rydberg Ensembles

Chris Nill<sup>1</sup>, Kay Brandner<sup>2</sup>, Beatriz Olmos<sup>1,2</sup>, Federico Carollo<sup>1</sup>, and Igor Lesanovsky<sup>1,2</sup>

<sup>1</sup>*Institut für Theoretische Physik, Universität Tübingen, Auf der Morgenstelle 14, 72076 Tübingen, Germany*

<sup>2</sup>*School of Physics and Astronomy and Centre for the Mathematics and Theoretical Physics of Quantum Non-Equilibrium Systems, The University of Nottingham, Nottingham NG7 2RD, United Kingdom*

 (Received 16 June 2022; accepted 7 November 2022; published 9 December 2022)

When atoms are excited to high-lying Rydberg states they interact strongly with dipolar forces. The resulting state-dependent level shifts allow us to study many-body systems displaying intriguing nonequilibrium phenomena, such as constrained spin systems, and are at the heart of numerous technological applications, e.g., in quantum simulation and computation platforms. Here, we show that these interactions also have a significant impact on dissipative effects caused by the inevitable coupling of Rydberg atoms to the surrounding electromagnetic field. We demonstrate that their presence modifies the frequency of the photons emitted from the Rydberg atoms, making it dependent on the local neighborhood of the emitting atom. Interactions among Rydberg atoms thus turn spontaneous emission into a many-body process which manifests, in a thermodynamically consistent Markovian setting, in the emergence of collective jump operators in the quantum master equation governing the dynamics. We discuss how this collective dissipation—stemming from a mechanism different from the much studied superradiance and subradiance—accelerates decoherence and affects dissipative phase transitions in Rydberg ensembles.

DOI: [10.1103/PhysRevLett.129.243202](https://doi.org/10.1103/PhysRevLett.129.243202)

*Introduction.*—Rydberg gases allow us to explore the interplay between strong interactions, external driving imposed by external fields, and dissipation. This has led to a whole host of theoretical and experimental works, investigating, for example, dissipative phase transitions, the dynamics of epidemic spreading and critical phenomena [1–6], as well as the dissipative preparation of correlated quantum states [7–11]. Dissipation typically manifests through two processes, which are decoherence (of quantum superposition) and radiative decay [12–15]. Decoherence leads to a gradual decay of quantum superposition that is formed between the high-lying Rydberg state and the atomic ground state from which the Rydberg state is excited. This process can be controlled by the phase coherence of the excitation laser and by the temperature of the Rydberg gas. It is also influenced by strong interactions among Rydberg atoms [15–18], which can be exploited for designing single photon absorbers and emitters [19–23]. Radiative decay, on the other hand, is a ubiquitous process which is caused by the coupling of the atomic dipole to the electromagnetic field. This results in the spontaneous emission of a photon from a Rydberg excited atom and a concomitant quantum jump from the Rydberg state to a low-lying electronic state, e.g., the ground state.

When considering ensembles of atoms, their coupling to the radiation field [24,25] can lead to collective behavior as pointed out by Dicke in his seminal work [26]. This emerges when the typical distance between the atoms becomes comparable to the wavelength of the emitted radiation.

In this case it is no longer possible to trace an emitted photon back to a specific atom. This loss of which-way information results in quantum interference that ultimately promotes this dissipation from a single-atom to a many-atom process. A striking consequence of this is the appearance of subradiant collective states whose lifetime may exceed that of single atoms by orders of magnitude [27–34]. In typical experiments, Rydberg atoms are separated by several micrometers. This is significantly larger than the wavelength for transitions to low-lying states, which is on the order of a hundred nanometers. Radiative decay is therefore here not expected to acquire a collective character and is typically modeled as a single-atom process. Note, that superradiance and subradiance can nevertheless occur and have been investigated in Rydberg gases [35–38]. However, in these studies the considered radiative transitions take place among Rydberg states and the associated wavelengths are on the order of millimeters to centimeters [39].

In this Letter, we demonstrate that strong interactions in Rydberg gases can nevertheless be responsible for another mechanism underlying collective dissipation. The fundamental observation is that the frequency of a photon that is spontaneously emitted from a decaying Rydberg atom depends on the state of the neighborhood of the emitting atom [cf. Figs. 1(a) and 1(b)]. We unveil this effect and analyze its consequences in a simple setting, permitting for the exact derivation of the Markovian quantum master equation of the Rydberg gas which, as we discuss, features many-body jump operators. We show that the ensuing dissipation accelerates decoherence and that it further

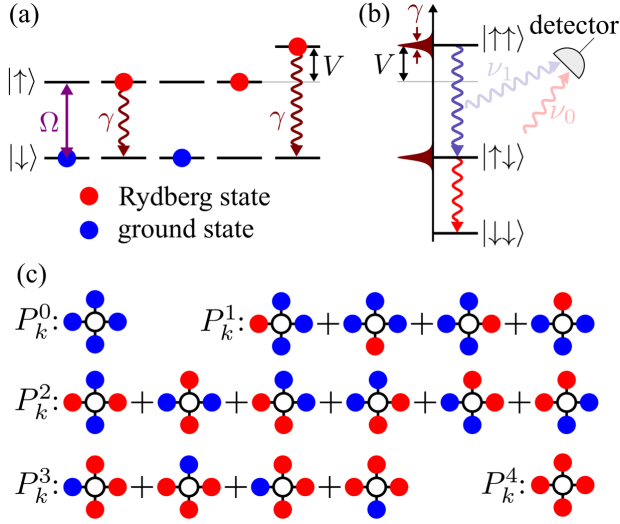


FIG. 1. Rydberg atoms and collective dissipation. (a) One-dimensional lattice gas of interacting atoms resonantly driven by a laser with Rabi frequency  $\Omega$ . Neighboring atoms interact with interaction strength  $V$  when simultaneously excited to their Rydberg state  $|\uparrow\rangle$ . Rydberg states decay under the emission of a photon to the ground state  $|\downarrow\rangle$  at rate  $\gamma$ . (b) Decay in a system of two atoms. When the interaction strength  $V$  is larger than the natural linewidth  $\gamma$  it is possible to discern whether a decaying Rydberg atom had an excited neighboring atom or not. This information can be inferred from the frequency of the emitted photon:  $\nu_1$ , excited neighboring atom;  $\nu_0$ , neighboring atom in the ground state. (c) Graphical representation of projectors  $P_k^\xi$  which project on the subspace where the neighborhood of a reference atom (empty circle) contains  $\xi$  excited atoms (in two dimensions). Because of the strong nearest-neighbor interaction an emitted photon carries information on the subspace from which the emission took place, leading to collective jump operators.

impacts on nonequilibrium phase transitions occurring in the stationary state of driven Rydberg gases. This collective state-dependent decay mechanism should be observable in (precision) experiments and is important for a thermodynamically consistent and faithful modeling of noise and error sources in quantum computers and simulators based on Rydberg atoms.

*Interacting Rydberg gas in an electromagnetic field.*—To illustrate the abovementioned effect we focus on a simple model of a Rydberg gas. The atoms are placed on the sites of a  $d$ -dimensional hypercubic lattice, labeled by the position vectors  $\mathbf{r}_k$ . Each atom is effectively described as a two-level (spin) system [see sketch in Fig. 1(a)], with ground state  $|\downarrow\rangle$  and Rydberg state  $|\uparrow\rangle$  separated by an energy difference  $\omega_a$ . We also assume for simplicity that the atoms only interact with their nearest neighbors with coupling strength  $V$  [see Fig. 1(a)]. This is accounted for by the Hamiltonian,

$$H_{\text{atom}} = \omega_a \sum_k n_k + \frac{V}{2} \sum_{|k-m|=1} n_k n_m, \quad (1)$$

where  $n_k = |\uparrow_k\rangle\langle\uparrow_k|$  is the projector on the Rydberg state of the atom located at position  $\mathbf{r}_k$ .

The atoms are immersed in an electromagnetic radiation field, described by the Hamiltonian,

$$H_{\text{rad}} = \sum_{\mathbf{q},s} \omega_{\mathbf{q}} a_{\mathbf{q}s}^\dagger a_{\mathbf{q}s}. \quad (2)$$

Here,  $a_{\mathbf{q}s}$  and  $a_{\mathbf{q}s}^\dagger$  are the annihilation and creation operators of a photon mode with momentum  $\mathbf{q}$ , polarization  $s$ , and energy  $\omega_{\mathbf{q}} = c|\mathbf{q}|$  ( $c$  is the speed of light). The dipole coupling between the atoms and the electromagnetic field modes is determined by the interaction Hamiltonian:

$$H_{\text{int}} = \sum_{k,\mathbf{q},s} (g_{\mathbf{q}s} a_{\mathbf{q}s}^\dagger e^{i\mathbf{q}\cdot\mathbf{r}_k} + \text{H.c.}) (\sigma_k^+ + \sigma_k^-). \quad (3)$$

Here,  $\sigma_k^+ = (\sigma_k^-)^\dagger = |\uparrow_k\rangle\langle\downarrow_k|$  is the atomic raising operator for the atom located at  $\mathbf{r}_k$ . The coupling constant  $g_{\mathbf{q}s} = \sqrt{(\omega_{\mathbf{q}}/2\epsilon_0\mathcal{V})(\mathbf{d}\cdot\mathbf{e}_s)}$  depends on the atomic transition dipole moment  $\mathbf{d}$ , the unit polarization vector  $\mathbf{e}_s$ , the vacuum permittivity  $\epsilon_0$ , and the quantization volume  $\mathcal{V}$ . Note that a variant of this model was considered also in Refs. [40,41], to study superradiance in the presence of interactions.

Our aim is to integrate out the electromagnetic field modes in order to obtain a quantum master equation that describes the open quantum dynamics of the atomic ensemble. We follow a procedure analogous to the usual one developed for the description of noninteracting atoms immersed in the radiation field (see, e.g., Refs. [24,25]). First, we rotate into the interaction picture with respect to the atom and radiation degrees of freedom via the unitary transformation  $U = \exp[it(H_{\text{atom}} + H_{\text{rad}})]$ . Because of the Rydberg interactions, atomic operators acquire an operator-valued phase which depends on the neighborhood of the considered atom, e.g.,

$$U \sigma_k^+ U^\dagger = \sigma_k^+ \exp(i\omega_a t) \exp\left(iVt \sum_{\xi=0}^{2d} \xi P_k^\xi\right). \quad (4)$$

Here,  $\xi \in \{0, 1, \dots, 2d\}$  and  $P_k^\xi$  is the projector on the subspace containing exactly  $\xi$  excited atoms in the neighborhood of atom  $k$  [see Fig. 1(c)]. Similar structures emerge, for example, in the so-called PXP model or the quantum hard-squares model, which describe strongly interacting Rydberg gases [42,43].

As derived in the Supplemental Material [44], after the Born-Markov and rotating-wave approximations, the quantum master equation reads (in the original lab frame):

$$\dot{\rho} = -i[H_{\text{atom}}, \rho] + \gamma \sum_k \left[ \sum_{\xi=0}^{2d} P_k^\xi \sigma_k^- \rho \sigma_k^+ P_k^\xi - \frac{1}{2} \{n_k, \rho\} \right], \quad (5)$$

where  $\gamma = (|\mathbf{d}|^2 \omega_a^3)/(3\pi c^3 \epsilon_0)$  is the single-atom decay rate. Note that for the rotating-wave approximation to be valid, the nearest-neighbor interaction strength  $V$  must be much larger than  $\gamma$ . Moreover, we have assumed that  $\omega_a \gg V$ , which allows us to neglect corrections to the spontaneous emission rate originating from the interaction shift of the atomic levels in the presence of neighboring excitations, which are of order  $\omega_a/V$ . Finally, note that we consider the separation between neighboring atoms to be much larger than the transition wavelength  $\lambda = 2\pi c/\omega_a$ . This allows us to neglect the effect of coherent dipole-dipole interactions and collective dissipation (i.e., superradiance and subradiance) induced by the radiation field. These conditions are typically met in current Rydberg quantum simulators using optical tweezer arrays. For example, in the experiment reported in Ref. [52], one finds for rubidium-87 atoms (principal quantum number  $n = 75$ , lattice constant  $10 \mu\text{m}$ ,  $C_6$  coefficient  $C_6 = \hbar \times 2\pi \times 1.947 \text{ GHz } \mu\text{m}^6$ ):  $\omega_a \approx 10^{15} \text{ Hz}$ ,  $V = \hbar \times 2\pi \times 2 \times 10^6 \text{ Hz}$ , and  $\gamma = 6 \times 10^3 \text{ Hz}$ .

From the master equation (5) one can read off that an atom at position  $\mathbf{r}_k$  has  $2d + 1$  different decay channels, where  $d$  is the dimension of the hypercubic lattice on which the atoms are positioned. Each of these channels, which is represented by the collective many-body jump operator  $L_k^c = \sqrt{\gamma} P_k^\xi \sigma_k^-$ , corresponds to a different number of excited atoms  $\xi$  in the atom's neighborhood, and can be associated to a different frequency of the emitted photons,  $\nu_\xi = \omega_a + \xi V$  [see Fig. 1(b)]. The many-body operators  $L_k^c$  are also consistent with thermodynamic considerations. While we treat the background radiation field as an effective zero-temperature reservoir here, which is well justified since the atomic energy scale  $\omega_a$  is typically much larger than the temperatures encountered in quantum-optical experiments, it is in principle straightforward to extend our approach to thermal environments with finite inverse temperature  $\beta$ . One would then expect the Gibbs state  $\propto \exp[-\beta(H_{\text{atom}})]$  to be a stationary state of the corresponding master equation. This condition, which is indeed met in our many-body approach, is also both sufficient and necessary for consistency with the second law of thermodynamics, at least in situations where the standard weak-coupling, Born-Markov and rotating-wave approximations are applicable [53,54]. On the other hand, a simpler model in which each atom would feature a single decay channel, represented by a jump operator  $L_k^s = \sqrt{\gamma} \sigma_k^-$  that does not account for interactions between atoms, would lead to a nonthermal stationary state at finite temperatures and thus, in general, to violations of the second law; see also Ref. [55].

*Decoherence dynamics.*—In order to analyze the impact of collective jump operators versus the conventionally employed single-atom decay, we consider an atomic ensemble that is initially prepared in the state  $|\Psi_0\rangle = (1/2)^{N/2} \otimes_k [|\downarrow\rangle_k + |\uparrow\rangle_k]$ . Experimentally, such a product state can be prepared in an interacting system by a

strong laser pulse whose Rabi frequency  $\Omega$  is much larger than the interaction strength  $V$ . We study the evolution of the average single-atom (Rydberg state–ground state) coherence, which can be measured experimentally [56], and which we decompose as

$$X(t) = \frac{1}{N} \sum_k \langle \sigma_k^- \rangle(t) = \frac{1}{N} \sum_{k,\xi} \langle P_k^\xi \sigma_k^- \rangle(t) = \sum_\xi X_\xi(t).$$

The evolution equation of the expectation values  $X_\xi$  is readily obtained [44]. For the collective dissipation, described by Eq. (5), we obtain

$$\dot{X}_\xi^c = -\left(i\omega_a + \frac{\gamma}{2}\right) X_\xi^c - \xi(\gamma + iV) X_\xi^c,$$

while for the conventionally employed single-atom decay,

$$\dot{X}_\xi^s = -\left(i\omega_a + \frac{\gamma}{2}\right) X_\xi^s - \xi(\gamma + iV) X_\xi^s + \gamma(\xi + 1) X_{\xi+1}^s,$$

where we use the convention  $X_{2d+1}^s = 0$ . These equations can be exactly integrated with initial condition  $X_\xi^{s/c}(0) = (1/N) \sum_k \langle \Psi_0 | P_k^\xi \sigma_k^- | \Psi_0 \rangle = 2^{-2d-1} \binom{2d}{\xi}$  [44]. Here, we focus on the short-time behavior, which already displays a qualitative difference between collective dissipation and single-body decay:

$$\begin{aligned} |X^s(t)| &\approx \frac{1}{2} - \frac{1}{4} \gamma t + \frac{\gamma^2 - 2dV^2}{16} t^2, \\ |X^c(t)| &\approx \frac{1}{2} - \frac{2d+1}{4} \gamma t + \frac{[(2d+1)^2 + 2d]\gamma^2 - 2dV^2}{16} t^2. \end{aligned}$$

For single-atom decay the initial drop of the coherence from its initial value  $1/2$  is independent of the system geometry. The first collective contribution in  $|X^s(t)|$  emerges from the interaction of an atom with its neighbors, which involves the interaction strength  $V$  and the coordination number  $2d$  and is thus not of dissipative nature. In contrast, for the case of collective decay, already the leading term is dependent on the coordination number. This shows that collective dissipation notably accelerates the decoherence process as compared to the single-atom case. We briefly discuss the effect of collective dissipation on other coherence observables and on quantum correlations in Ref. [44].

This effect should be even more dramatic in a continuous gas. Here, the initial rate of decoherence is proportional to the number of atoms  $N_{\text{int}}$ , with which a given reference atom interacts strongly enough so that the concomitant energy shift exceeds the single-atom decay rate  $\gamma$ . For a homogeneous atomic gas with density  $\rho_0$  and Rydberg states that are interacting with a van der Waals potential [39],  $V_{\text{vdW}}(r) = C_6/r^6$ , this number of atoms scales as

$N_{\text{int}} \sim \varrho_0(|C_6|/\gamma)^{d/6}$  and thus the collective decoherence rate should scale as  $\gamma_c \sim \gamma \varrho_0(C_6/\gamma)^{d/6}$ .

*Stationary state of a laser-driven Rydberg gas.*—The stationary state of the dynamics considered so far is the one devoid of any Rydberg excitation, since the system is only coupled with an effectively zero-temperature reservoir. In the following, we are interested in exploring the stationary state that emerges when (collective) radiative decay competes with external laser driving. To include the excitation laser (with frequency  $\omega_l$ , Rabi frequency  $\Omega$ , and detuning  $\Delta = \omega_a - \omega_l$ ) we consider master equation (5) with the modified atomic Hamiltonian:

$$H_{\text{atom}} \rightarrow H_{\text{atom}} + \sum_k [\Omega \sigma_k^x + (\Delta - \omega_a) n_k]. \quad (6)$$

This is actually an *ad hoc* construction, given that the master equation has to be derived using the modified Hamiltonian. However, this approach is currently the standard one for incorporating coherent laser excitation, interaction, and dissipation in interacting Rydberg gases [4,12,15,57]. Our expectation at this point is that its analysis will reveal which quantitative and qualitative changes to the stationary state—caused by collective jump operators—one may expect.

We first perform a mean field analysis. Following the treatment of Ref. [2], this leads to the mean field equations of motion:

$$\begin{aligned} \dot{n} &= \Omega s_y - \gamma n, \\ \dot{s}_x &= -\Delta s_y - \frac{\gamma}{2}(4dn + 1)s_x - 2dVns_y, \\ \dot{s}_y &= -\Delta s_x - \frac{\gamma}{2}(4dn + 1)s_y + 2dVns_x - \Omega(4n - 2). \end{aligned} \quad (7)$$

Here,  $n = \langle n_k \rangle$ ,  $s_x = \langle \sigma_x^k \rangle$ , and  $s_y = \langle \sigma_y^k \rangle$ , and translation invariance is assumed throughout. A noteworthy aspect of these equations is their dependence on the dimension  $d$ . In the contribution due to interactions, the latter enters through the combination  $2dV$ , with  $2d$  being the coordination number of the  $d$ -dimensional hypercubic lattice. Therefore, different dimensions simply lead to a rescaling of the mean field interaction. This is not the case for the collective decay which results in terms proportional to  $\gamma(4dn + 1)$ , which does not amount to a simple rescaling when changing dimensionality. This becomes visible in the stationary state phase diagram displayed in Fig. 2. In the main figure we show the number of stable stationary mean field solutions. While for most parameters there is merely one solution, there exists a region for which two stationary solutions emerge. This bistability, extensively discussed in the literature, e.g., in Refs. [2,4,58], is seen in the inset. There we show the stationary Rydberg excitation density  $n_{\text{ss}}^c$  as obtained from the mean field equations (7) after setting the time derivatives to zero and solving for  $n$ . From a

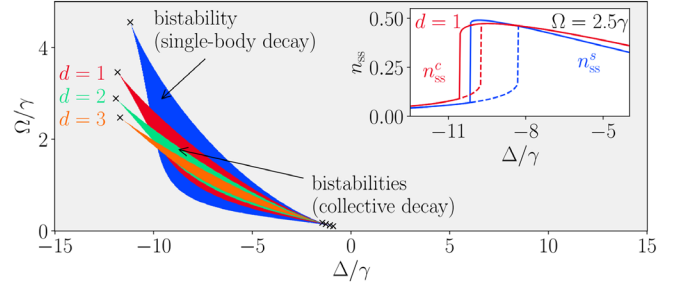


FIG. 2. Bistability region in the mean field phase diagram in the presence of single-atom and collective decay. In the gray region the stationary state of the mean field equations is unique. In the colored region, whose shape depends on the dimension  $d$ , two stationary solutions exist. The cusps culminate in critical points, which are marked by crosses. The inset shows a cut of the stationary state density through the bistability region, taken at  $\Omega = 2.5\gamma$ . The red (blue) curves show the stationary Rydberg excitation density  $n_{\text{ss}}^c$  ( $n_{\text{ss}}^s$ ), where the superscript  $c$  ( $s$ ) refers to collective (single-atom) decay of collective (single-atom) decay. Solid and dashed lines mark the two stationary solutions. We have set  $dV = 10\gamma$ . The mean field equations for  $n_{\text{ss}}^c$  are in Eq. (7) while those for  $n_{\text{ss}}^s$  are given in Ref. [44].

dynamical perspective bistability typically manifests in intermittency of the quantum jump statistics [1,59,60]. The important aspect here is that the size and shape of this region strongly depend on the dimensionality, which is not the case when single-body decay is considered where one can simply rescale the interaction strength.

To complement the mean field analysis we numerically calculate the stationary state of a small one-dimensional chain containing either  $N = 4$  or  $N = 8$  atoms. Qualitatively, both single-body and collective decay yield similar results, which are displayed in Fig. 3. For negative detunings  $\Delta$ —where the mean field analysis predicts bistable behavior—there is, however, a substantial quantitative difference. For example, the excitation density under collective dissipation can exceed the one predicted by single-atom decay by more than a factor 2. This indicates that the bistable or metastable (in low dimensions) regions indeed are located in different regions of the parameter space, as the mean field result suggests. Note that these features persist in the presence of weak laser phase noise [44].

*Conclusions and future directions.*—In this Letter, we have studied the radiative decay of an interacting Rydberg gas. We have considered a rather simplified scenario, in which Rydberg atoms interact with nearest-neighbor interaction  $V$ , whose value exceeds that of the emission linewidth  $\gamma$ . Realistic interactions have a gradually decaying tail and there will be distances in which the interaction strength between the atoms becomes comparable with the decay rate. Here it is no longer possible to perform a rotating-wave approximation and the master equation becomes explicitly time dependent. Moreover, it would be interesting to include the laser driving systematically in



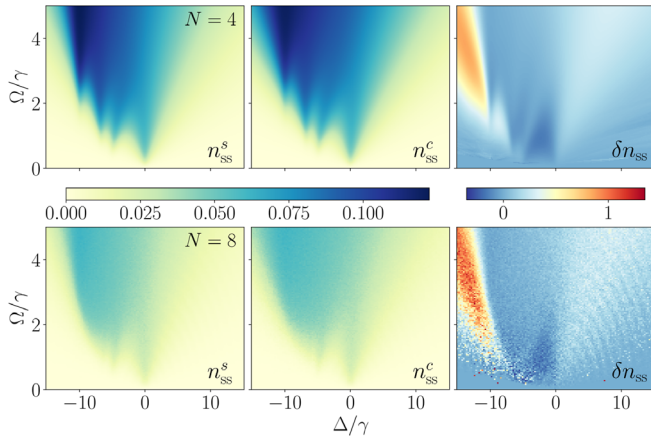


FIG. 3. Stationary state of a  $d=1$  chain with periodic boundaries. Shown is the stationary density of Rydberg excitations as a function of the laser detuning  $\Delta$  and the Rabi frequency  $\Omega$  with  $V=10\gamma$  in the presence of single-body decay ( $n_{ss}^s$ ) and collective many-body decay ( $n_{ss}^c$ ). The data are obtained by solving Eq. (5) with Hamiltonian (6). In the rightmost column we show the relative difference between the two densities,  $\delta n_{ss} = (n_{ss}^c - n_{ss}^s)/n_{ss}^s$ . Significant deviations are visible for negative detunings in the region where bistable behavior is predicted by the mean field analysis. To estimate the steady state we average over 100 linearly spaced data points in the interval  $[4.75\gamma t, 5.00\gamma t]$ . The oscillations visible in the region  $\Delta/\gamma > 0$  are a finite time effect. The data for  $N=4$  are obtained by exact diagonalization, while the  $N=8$  data were calculated using continuous-time quantum jump Monte Carlo averaged over 300 trajectories.

the derivation of the master equation for the atomic system, e.g., by using the Floquet-Lindblad approach, which makes it possible to accommodate strong periodic driving fields in a thermodynamically consistent way [61]. For the sake of simplicity, we have focused on an *ad hoc* approach in this Letter, where the driving is incorporated only in the unitary part of the master equation, as is currently standard quantum optics.

In order to experimentally probe the impact of collective effects it would be desirable to investigate strongly interacting Rydberg lattice systems that allow us to observe dissipative dynamics over many emission cycles. This should be, for example, possible in trapped Rydberg ion systems [62,63], which provide trapping of ground and Rydberg states alike and also offer the opportunity to continuously cool external degrees of freedom that may be heated from spontaneous emission.

The research leading to these results has received funding from the Wissenschaftler-Rückkehrprogramm GSO/CZS of the Carl-Zeiss-Stiftung and the German Scholars Organization e.V., through the Deutsche Forschungsgemeinschaft (DFG, German Research Foundation) under Projects No. 435696605 and No. 449905436, as well as through the Research Unit FOR 5413/1, Grant No. 465199066. We also acknowledge support from the Baden-Württemberg

Stiftung through Project No. BWST\_ISF2019-23. This work was supported by the University of Nottingham and the University of Tübingen's funding as part of the Excellence Strategy of the German Federal and State Governments, in close collaboration with the University of Nottingham. K. B. acknowledges support from the University of Nottingham through a Nottingham Research Fellowship. This work was supported by the Medical Research Council (Grant No. MR/S034714/1) and the Engineering and Physical Sciences Research Council (Grant No. EP/V031201/1). F. C. is indebted to the Baden-Württemberg Stiftung for the financial support by the Eliteprogramme for Postdocs.

- [1] N. Malossi, M. M. Valado, S. Scotto, P. Huillery, P. Pillet, D. Ciampini, E. Arimondo, and O. Morsch, *Phys. Rev. Lett.* **113**, 023006 (2014).
- [2] M. Marcuzzi, E. Levi, S. Diehl, J. P. Garrahan, and I. Lesanovsky, *Phys. Rev. Lett.* **113**, 210401 (2014).
- [3] A. Urvoy, F. Ripka, I. Lesanovsky, D. Booth, J. P. Shaffer, T. Pfau, and R. Löw, *Phys. Rev. Lett.* **114**, 203002 (2015).
- [4] F. Letscher, O. Thomas, T. Niederprüm, M. Fleischhauer, and H. Ott, *Phys. Rev. X* **7**, 021020 (2017).
- [5] R. Gutiérrez, C. Simonelli, M. Archimi, F. Castellucci, E. Arimondo, D. Ciampini, M. Marcuzzi, I. Lesanovsky, and O. Morsch, *Phys. Rev. A* **96**, 041602(R) (2017).
- [6] S. Helmrich, A. Arias, G. Lochead, T. Wintermantel, M. Buchhold, S. Diehl, and S. Whitlock, *Nature (London)* **577**, 481 (2020).
- [7] B. Kraus, H. P. Büchler, S. Diehl, A. Kantian, A. Micheli, and P. Zoller, *Phys. Rev. A* **78**, 042307 (2008).
- [8] A. W. Carr and M. Saffman, *Phys. Rev. Lett.* **111**, 033607 (2013).
- [9] M. Höning, D. Muth, D. Petrosyan, and M. Fleischhauer, *Phys. Rev. A* **87**, 023401 (2013).
- [10] D. Petrosyan, M. Höning, and M. Fleischhauer, *Phys. Rev. A* **87**, 053414 (2013).
- [11] M. Roghani and H. Weimer, *Quantum Sci. Technol.* **3**, 035002 (2018).
- [12] R. Lw, H. Weimer, J. Nipper, J. B. Balewski, B. Butscher, H. P. Bchler, and T. Pfau, *J. Phys. B* **45**, 113001 (2012).
- [13] M. Gärtner, S. Whitlock, D. W. Schönleber, and J. Evers, *Phys. Rev. Lett.* **113**, 233002 (2014).
- [14] M. Marcuzzi, J. Schick, B. Olmos, and I. Lesanovsky, *J. Phys. A* **47**, 482001 (2014).
- [15] E. Guardado-Sanchez, P. T. Brown, D. Mitra, T. Devakul, D. A. Huse, P. Schauß, and W. S. Bakr, *Phys. Rev. X* **8**, 021069 (2018).
- [16] F. Letscher, O. Thomas, T. Niederprüm, H. Ott, and M. Fleischhauer, *Phys. Rev. A* **95**, 023410 (2017).
- [17] A. Signoles, T. Franz, R. Ferracini Alves, M. Grtner, S. Whitlock, G. Zrn, and M. Weidemüller, *Phys. Rev. X* **11**, 011011 (2021).
- [18] P. Schultzen, T. Franz, S. Geier, A. Salzinger, A. Tebben, C. Hainaut, G. Zürn, M. Weidemüller, and M. Gärtner, *Phys. Rev. B* **105**, L020201 (2022).
- [19] F. Bariani, Y. O. Dudin, T. A. B. Kennedy, and A. Kuzmich, *Phys. Rev. Lett.* **108**, 030501 (2012).

- [20] Y. Dudin and A. Kuzmich, *Science* **336**, 887 (2012).
- [21] J. Honer, R. Löw, H. Weimer, T. Pfau, and H. P. Büchler, *Phys. Rev. Lett.* **107**, 093601 (2011).
- [22] C. Tresp, C. Zimmer, I. Mirgorodskiy, H. Gorniaczyk, A. Paris-Mandoki, and S. Hofferberth, *Phys. Rev. Lett.* **117**, 223001 (2016).
- [23] N. Stiesdal, H. Busche, K. Kleinbeck, J. Kumlin, M. G Hansen, H. P. Büchler, and S. Hofferberth, *Nat. Commun.* **12**, 4328 (2021).
- [24] R. H. Lehmburg, *Phys. Rev. A* **2**, 883 (1970).
- [25] D. F. V. James, *Phys. Rev. A* **47**, 1336 (1993).
- [26] R. H. Dicke, *Phys. Rev.* **93**, 99 (1954).
- [27] A. Asenjo-Garcia, M. Moreno-Cardoner, A. Albrecht, H. J. Kimble, and D. E. Chang, *Phys. Rev. X* **7**, 031024 (2017).
- [28] J. A. Needham, I. Lesanovsky, and B. Olmos, *New J. Phys.* **21**, 073061 (2019).
- [29] O. Rubies-Bigorda, V. Walther, T. L. Patti, and S. F. Yelin, *Phys. Rev. Res.* **4**, 013110 (2022).
- [30] Y.-X. Zhang, C. Yu, and K. Mølmer, *Phys. Rev. Res.* **2**, 013173 (2020).
- [31] G. Facchinetti, S. D. Jenkins, and J. Ruostekoski, *Phys. Rev. Lett.* **117**, 243601 (2016).
- [32] W. Guerin, M. O. Araújo, and R. Kaiser, *Phys. Rev. Lett.* **116**, 083601 (2016).
- [33] J. Rui, D. Wei, A. Rubio-Abadal, S. Hollerith, J. Zeiher, D. M. Stamper-Kurn, C. Gross, and I. Bloch, *Nature (London)* **583**, 369 (2020).
- [34] G. Ferioli, A. Glicenstein, L. Henriët, I. Ferrier-Barbut, and A. Browaeys, *Phys. Rev. X* **11**, 021031 (2021).
- [35] M. Gross, P. Goy, C. Fabre, S. Haroche, and J. M. Raimond, *Phys. Rev. Lett.* **43**, 343 (1979).
- [36] T. Wang, S. F. Yelin, R. Côté, E. E. Eyler, S. M. Farooqi, P. L. Gould, M. Koštrun, D. Tong, and D. Vrinceanu, *Phys. Rev. A* **75**, 033802 (2007).
- [37] L. Hao, Z. Bai, J. Bai, S. Bai, Y. Jiao, G. Huang, J. Zhao, W. Li, and S. Jia, *New J. Phys.* **23**, 083017 (2021).
- [38] E. Suarez, P. Wolf, P. Weiss, and S. Slama, *Phys. Rev. A* **105**, L041302 (2022).
- [39] M. Saffman, T. G. Walker, and K. Mølmer, *Rev. Mod. Phys.* **82**, 2313 (2010).
- [40] S. P. Lukyanets and D. A. Bevezhenko, *Phys. Rev. A* **74**, 053803 (2006).
- [41] S. P. Lukyanets and D. A. Bevezhenko, *Opt. Spectrosc.* **111**, 727 (2011).
- [42] B. Sun and F. Robicheaux, *New J. Phys.* **10**, 045032 (2008).
- [43] I. Lesanovsky, *Phys. Rev. Lett.* **106**, 025301 (2011).
- [44] See Supplemental Material at <http://link.aps.org/supplemental/10.1103/PhysRevLett.129.243202>, which includes Refs. [45–51], for details.
- [45] H.-P. Breuer and F. Petruccione, *The Theory of Open Quantum Systems* (Oxford University Press, Oxford, 2007), 10.1093/acprof:oso/9780199213900.001.0001.
- [46] A. G. Redfield, *IBM J. Res. Dev.* **1**, 19 (1957).
- [47] R. M. Wilcox, *J. Math. Phys. (N.Y.)* **8**, 962 (1967).
- [48] J. Johansson, P. Nation, and F. Nori, *Comput. Phys. Commun.* **183**, 1760 (2012).
- [49] J. Johansson, P. Nation, and F. Nori, *Comput. Phys. Commun.* **184**, 1234 (2013).
- [50] J. Cresser and C. Facer, *Opt. Commun.* **283**, 773 (2010).
- [51] H. Levine, A. Keesling, A. Omran, H. Bernien, S. Schwartz, A. S. Zibrov, M. Endres, M. Greiner, V. Vuletić, and M. D. Lukin, *Phys. Rev. Lett.* **121**, 123603 (2018).
- [52] P. Scholl, M. Schuler, H. J. Williams, A. A. Eberharter, D. Barredo, K.-N. Schymik, V. Lienhard, L.-P. Henry, T. C. Lang, T. Lahaye *et al.*, *Nature (London)* **595**, 233 (2021).
- [53] H. Spohn, *J. Math. Phys. (N.Y.)* **19**, 1227 (1978).
- [54] K. Brandner and U. Seifert, *Phys. Rev. E* **93**, 062134 (2016).
- [55] A. Levy and R. Kosloff, *Europhys. Lett.* **107**, 20004 (2014).
- [56] G. Semeghini, H. Levine, A. Keesling, S. Ebadi, T. T. Wang, D. Bluvstein, R. Verresen, H. Pichler, M. Kalinowski, R. Samajdar *et al.*, *Science* **374**, 1242 (2021).
- [57] M. Morgado and S. Whitlock, *AVS Quantum Sci.* **3**, 023501 (2021).
- [58] T. E. Lee, H. Häffner, and M. C. Cross, *Phys. Rev. A* **84**, 031402(R) (2011).
- [59] T. E. Lee, H. Häffner, and M. C. Cross, *Phys. Rev. Lett.* **108**, 023602 (2012).
- [60] C. Ates, B. Olmos, J. P. Garrahan, and I. Lesanovsky, *Phys. Rev. A* **85**, 043620 (2012).
- [61] R. Kosloff, *Entropy* **15**, 2100 (2013).
- [62] F. Schmidt-Kaler, T. Feldker, D. Kolbe, J. Walz, M. Müller, P. Zoller, W. Li, and I. Lesanovsky, *New J. Phys.* **13**, 075014 (2011).
- [63] C. Zhang, F. Pokorny, W. Li, G. Higgins, A. Pöschl, I. Lesanovsky, and M. Hennrich, *Nature (London)* **580**, 345 (2020).